Supplement of The Cryosphere, 13, 3007–3021, 2019
https://doi.org/10.5194/tc-13-3007-2019-supplement

The Cryosphere
Open Access

Supplement of

Decadal changes in the leading patterns of sea level pressure in the Arctic and their impacts on the sea ice variability in boreal summer

Nakbin Choi et al.

Correspondence to: Myong-In Lee (milee@unist.ac.kr)

Significance Test for Spatial Pattern Correlation

As the atmospheric circulation anomalies are varying in large spatial scale, each grid point is not regarded as an independent sample. According to Bretherton et al. (1999), the statistical significance test should be based on the effective sample size, which can be calculated as

$$N^* = N\,\frac{1 - r_1 r_2}{1 + r_1 r_2},$$

N is the total grid size, r_1 and r_2 is the autocorrelation applied to the spatial pattern shifted by one grid for the early and the recent pattern, respectively.

In the western hemisphere, the total sample size for pattern correlation is 17,620 (61 lat. x 289 lon. grids) and the effective sample size is much reduced as 6.05 (~ 7), due to the high coherency in the spatial pattern. When the sample size is 7, the correlation coefficient should be higher than 0.67 to be significant at the 90 %, 0.76 at the 95 %, and 0.88 at the 99 % confidence level, respectively.

List of Supplemental Material

Figure S1. Regression patterns of 850 hPa air temperature (°C). Dotted area indicates the statistically significant region at 95 % confidence level.

Figure S2. Temperature advection associated with AD (shaded, K day-1) shown with the wind at 500 hPa (vector, m/s) for (a) the early (1982-1997) and (b) the recent (1998-2017) period. Temperature advection is calculated by $\mathrm{V}' \cdot \nabla\bar{T} + \bar{V} \cdot \nabla T' + V' \cdot \nabla T'$, where $\bar{V}$ and $\bar{T}$ are time-mean 500 hPa wind and air temperature in each period, respectively, and. V' and T' are regressed wind and air temperature onto the AD index, respectively.

Figure S3. Surface heat flux changes associated with the summer AD in the past (1982-1997) and the recent (1998-2017) period. Sensible and latent heat fluxes are defined as positive for the upward. The AD index is reversed in sign before regression.

Figure S4. Leading EOF modes for the negative PDO phase before 1998. (a) is EOF1 and (b) is EOF2.

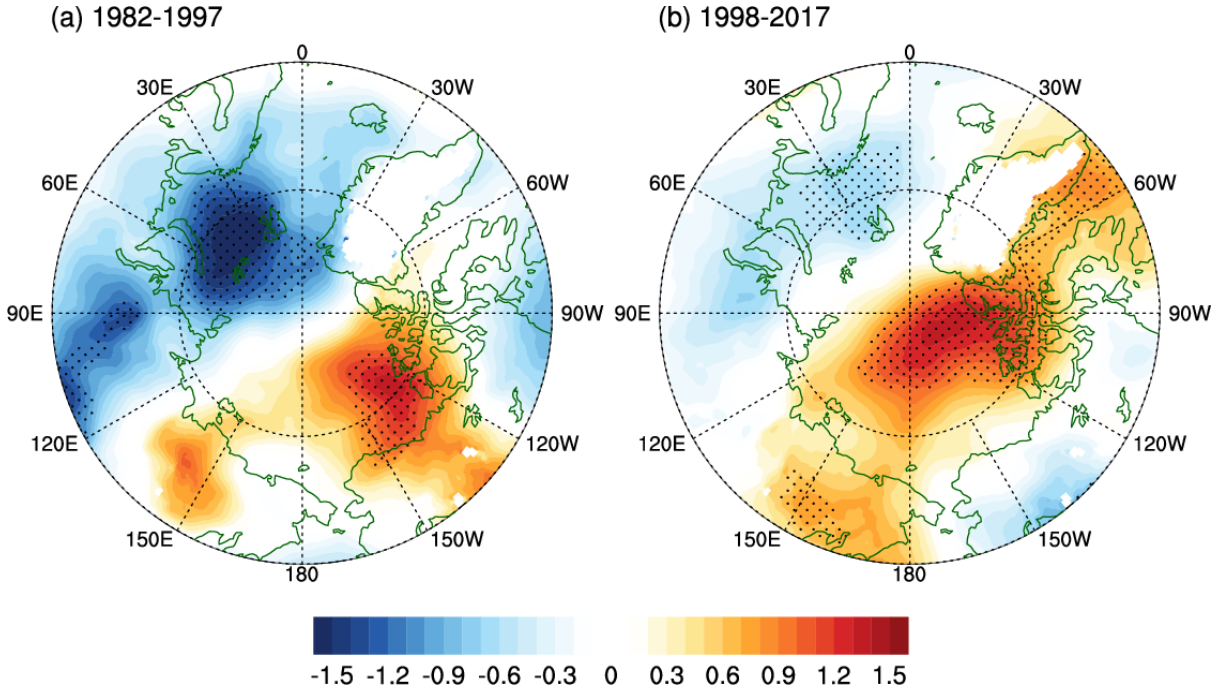

Figure S1. Regression patterns of 850 hPa air temperature (°C). Dotted area indicates the statistically significant region at 95 % confidence level.

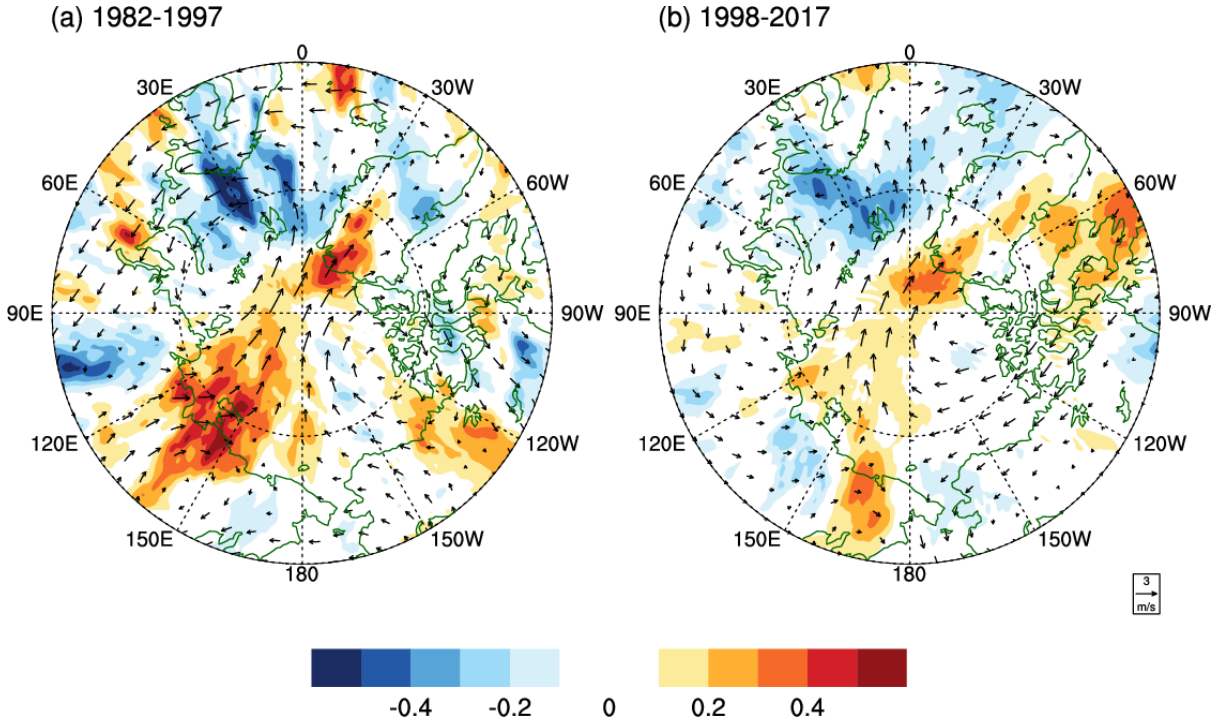

Figure S2. Temperature advection associated with AD (shaded, K day-1) shown with the wind at 500 hPa (vector, m/s) for (a) the early (1982-1997) and (b) the recent (1998-2017) period. Temperature advection is calculated by $\mathrm{V}' \cdot \nabla\bar{T} + \bar{V} \cdot \nabla T' + V' \cdot \nabla T'$, where $\bar{V}$ and $\bar{T}$ are time-mean 500 hPa wind and air temperature in each period, respectively, and. V' and T' are regressed wind and air temperature onto the AD index, respectively.

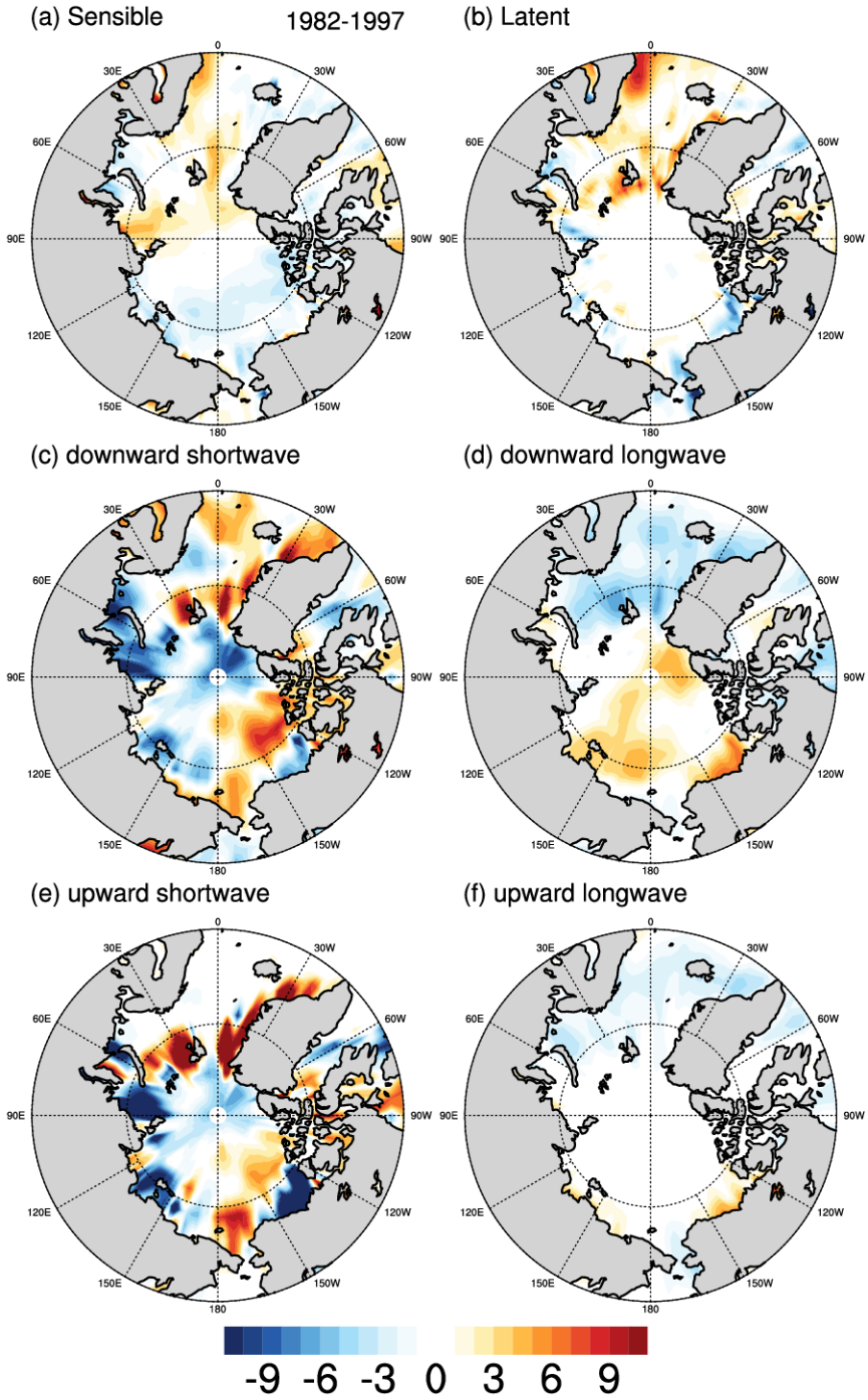

Figure S3. Surface heat flux changes associated with the summer AD in the past (1982-1997) and the recent (1998-2017) period. Sensible and latent heat fluxes are defined as positive for the upward. The AD index is reversed in sign before regression.

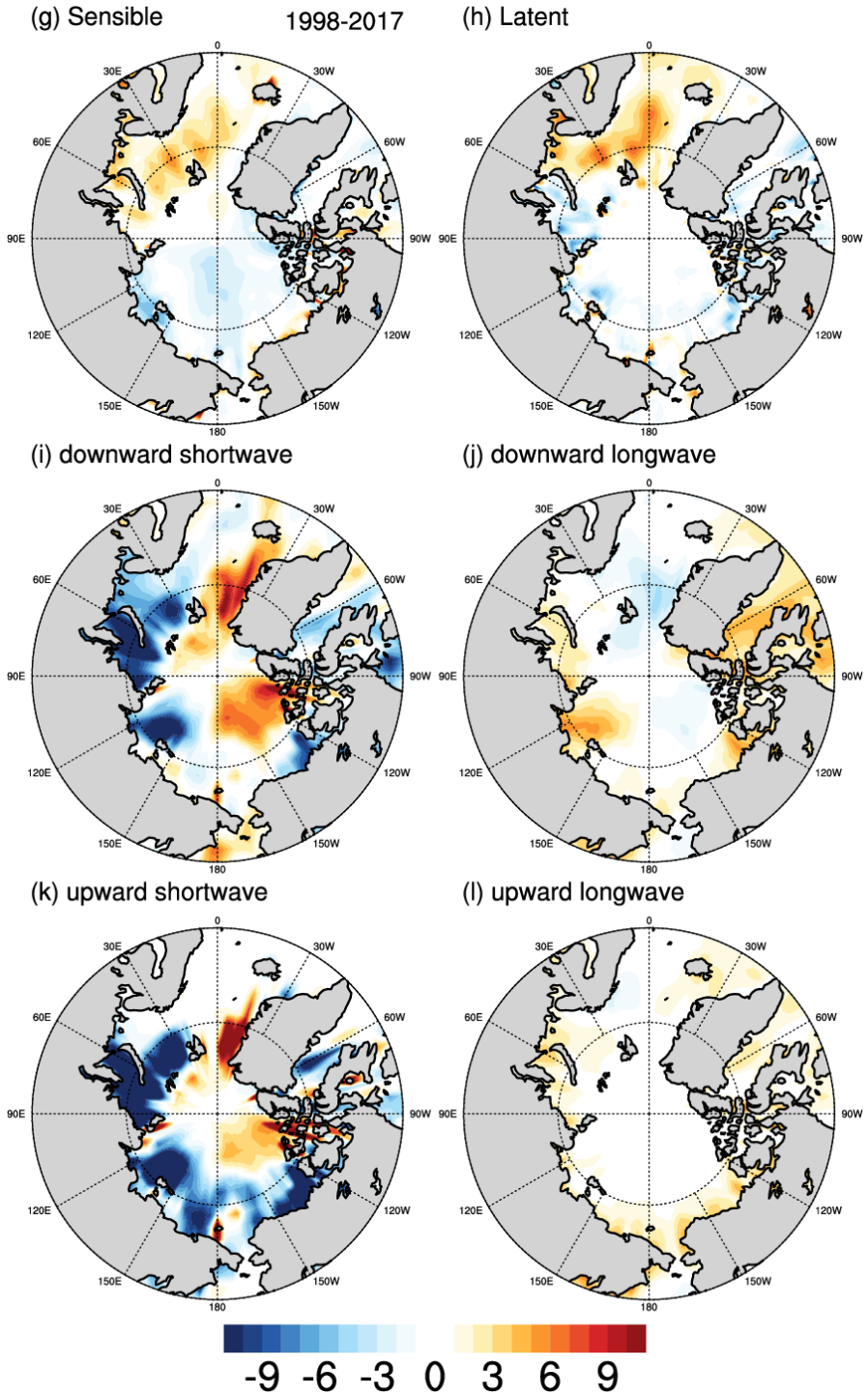

Figure S3. Continued.

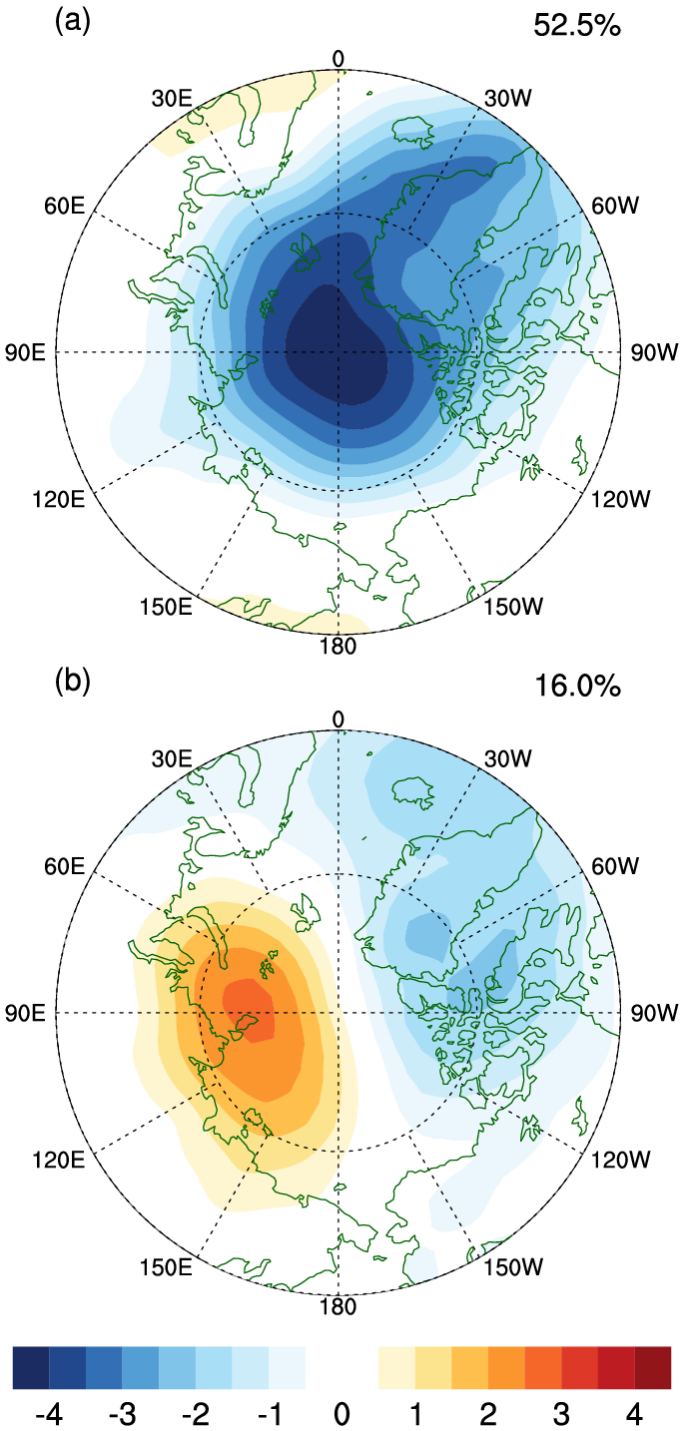

Figure S4. Leading EOF modes for the negative PDO phase before 1998. (a) is EOF1 and (b) is EOF2.